

DOI:10.13476/j.cnki.nsbdtk.2021.0084

任向轩,汤方平,徐莹,等.潜水搅拌机叶片安放角的性能[J].南水北调与水利科技(中英文),2021,19(4):805-813. REN X X, TANG F P, XU Y, et al. Performance analysis of blade angle of submersible agitator[J]. South-to-North Water Transfers and Water Science & Technology, 2021, 19(4): 805-813. (in Chinese)

# 潜水搅拌机叶片安放角的性能

任向轩<sup>1</sup>, 汤方平<sup>2</sup>, 徐莹<sup>1</sup>, 石丽建<sup>2</sup>, 尚晓君<sup>3</sup>

(1. 扬州大学电气与能源动力工程学院, 江苏 扬州 225009; 2. 扬州大学水利科学与工程学院, 江苏 扬州 225009; 3. 江苏省太湖地区水利工程管理处, 江苏 苏州 215128)

**摘要:**为研究潜水搅拌机在不同的叶片安放角度(-4°、-2°、0°、2°、4°)下对搅拌池内流场影响的差异,现分别对不同叶片安放角下的潜水搅拌机进行数值模拟并利用CFD后处理软件对所得的流场分析处理。根据数值模拟结果得出:在不同的叶片安放角下,潜水搅拌机流场的速度矢量图总体变化趋势一致且叶片安放角由-4°增大到4°,潜水搅拌机的搅拌效果越来越好;同时随着叶片安放角的增加,潜水搅拌机的轴功率、推力在不断地增大,叶片压力面的高压区也在逐渐地增大;相对于搅拌效果而言,在小转速下可以通过增大叶片安放角来增加潜水搅拌机的搅拌效果,在大转速下可以通过减小叶片安放角来控制潜水搅拌机的搅拌效果,以此达到有效节能的目的;为证明潜水搅拌机数值模拟结果的准确性,选取叶片安放角为0°时的情况进行了试验验证,为以后潜水搅拌机的研究提供一定的参考。

**关键词:**潜水搅拌机;叶片安放角;数值模拟;轴向流速

中图分类号:X703.3 文献标志码:A 开放科学(资源服务)标志码(OSID):



潜水搅拌机又称潜水推进器,被广泛应用于污水处理厂的工艺流程中<sup>[1-7]</sup>。近年来,随着计算机技术的发展,利用CFD软件模拟搅拌池内的流场变化,更明确地提供了一种理论支撑。正是这种数值模拟技术的出现,对潜水搅拌机的研究进入到了一个新的阶段。于是,研究人员从潜水搅拌机的设计参数、安装位置、调节转速等多方面入手,以求既可以提高潜水搅拌机的搅拌效果,又能达到有效节能的目的。

徐伟幸等<sup>[8-10]</sup>应用Fluent软件对潜水搅拌机搅拌流场进行模拟分析,提出了搅拌机叶轮的优化设计方案;刘晓满<sup>[11]</sup>将搅拌器的不同安装方案试验与数值模拟结果对比,得到了较优的安装方案和节能方案;徐顺等<sup>[12-13]</sup>将数值模拟与试验结果对比分析,提出了潜水搅拌机在选型过程中的影响因子和优化

方向,并对不同叶片间隙潜水搅拌机流场的变化分析比较,得到了最佳叶片间隙;张晓宁等<sup>[14]</sup>通过Fluent软件模拟计算,得出了潜水搅拌机不同水平安装角度对搅拌效果的影响;龚发云等<sup>[15]</sup>以CFD软件为计算平台,以潜水搅拌机桨叶为研究对象,探讨出了不同桨叶直径、桨叶转速及桨叶数对搅拌效果的影响规律;许乔<sup>[16]</sup>、徐莹等<sup>[17]</sup>基于轴流泵叶片设计方法,采用变环量流型设计潜水搅拌机叶片并进行数值模拟分析,发现设计的叶片有效提高了循环区的液流速度,增大了搅拌区域;朱桂华等<sup>[18]</sup>借助Fluent软件研究双潜水搅拌机在不同安装角度下的搅拌特性,并通过试验验证了数值模拟计算的有效性;施卫东等<sup>[19]</sup>利用Fluent软件对4种潜水搅拌机池形进行了数值模拟和分析,得出渐进圆管水池和直圆管水池两种池形是较为理想的污水搅拌水池。

收稿日期:2020-05-14 修回日期:2020-10-28 网络出版时间:2020-11-17

网络出版地址:https://kns.cnki.net/kcms/detail/13.1430.TV.20201117.0848.002.html

基金项目:江苏省自然科学基金(BK20190914);中国博士后科学基金(2019M661946);江苏省高校自然科学研究项目(19KJB570002);扬州市自然科学基金(YZ2018103);江苏省高校优势学科建设项目(PAPD)

作者简介:任向轩(1994—),男,山东济宁人,主要从事流体机械研究。E-mail:1215903365@qq.com

通信作者:汤方平(1964—),男,浙江金华人,教授,主要从事流体机械设计、复杂工程系统科学优化设计和泵站自动化等研究。E-mail:tangfp@yzu.edu.cn

到目前为止,前人<sup>[20-25]</sup>对潜水搅拌器的安装方案已经做了或多或少的研究。但是,潜水搅拌器叶片安放角对流场的影响是如何变化的,这方面的研究还没有涉及。因此,在前人所做研究的基础上,模拟计算叶片安放角对潜水搅拌器的性能影响。文中叶轮叶片安放角的改变通过在 TurboGrid 中绕 Y 轴旋转相应的角度来实现, Y 轴正向(顺时针)旋转 2°, 即叶片安放角调节 -2°(顺时针为负,逆时针为正), 以此类推。本文研究不同叶片安放角(-4°、-2°、0°、2°、4°)下搅拌池内流动特性,为根据搅拌要求和节能效果选择合适的叶片安放角度提供参考依据。

## 1 潜水搅拌器数值模拟

### 1.1 几何模型

搅拌池内的流场可近似认为是三维不可压缩流

场。池内所选用的液体为清水,搅拌水池的长(Z 方向)为 6 m,宽(X 方向)为 5 m,高(Y 方向)为 1.4 m,其中潜水搅拌器叶轮位于中部(Y 方向),距离池底为 0.7 m,电机尾部距离水池壁面为 175 mm,电机转速  $n=576 \text{ r/min}$ ,见图 1。选用的叶轮为采用变环量设计方法设计的潜水搅拌器叶片<sup>[16]</sup>,叶轮直径为 300 mm,叶片数为 3 片,轮毂比为 0.466 7,见图 2。

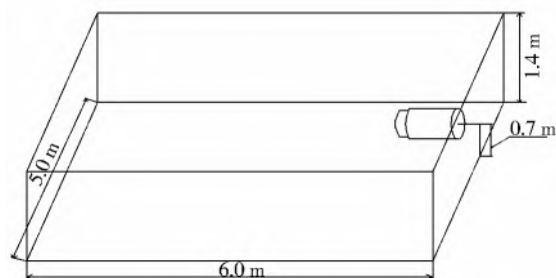


图 1 潜水搅拌器安装位置

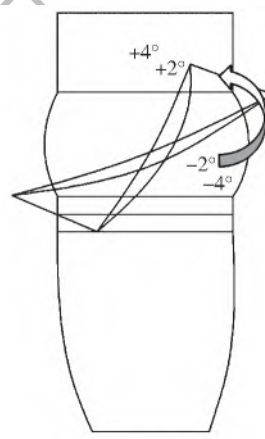
Fig. 1 Installation position diagram of submersible mixer



(a) 叶轮模型



(b) 叶轮实体模型



(c) 叶片安放角变化

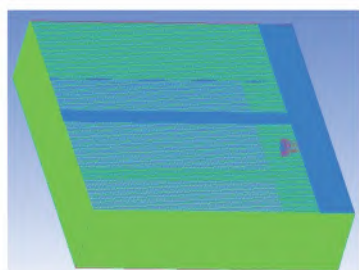
图 2 潜水搅拌器叶轮

Fig. 2 Impeller drawing of submersible agitator

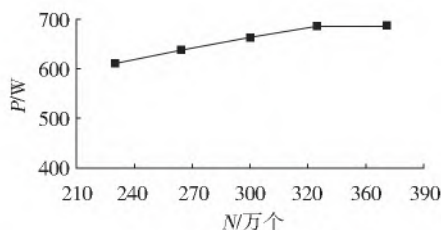
### 1.2 数学模型

网格划分是建立数学模型过程中重要的一步,网格质量的好坏更是会影响计算结果的成败。利用 ICEM 对水池部分进行结构化网格的划分,网格质量达到了 0.5 以上,对潜水搅拌器的叶轮部分利用 TurboGrid 进行网格划分,网格质量也达到了设计

要求。合适的网格数不仅可以使计算结果最优,而且可以大大节省计算时间,所以在数值模拟计算中网格无关性验证也是不可缺少的。经网格无关性分析,规定不同网格数下潜水搅拌器的功率改变量不超过 2% 为计算网格,确定最终网格数为 335 万,见图 3。



(a) 潜水搅拌器网格



(b) 网格无关性验证

图 3 潜水搅拌器网格划分

Fig. 3 Grid division of submersible agitator

将搅拌水池的四周墙壁和电机设置为固壁 (Wall), 水池液面近似为平面, 采用刚盖定理设置池面。叶轮设置相应的转速, 在动区域和静区域之间设置 interface 交界面, 其中: 静区域与静区域之间设置为静静交界面, 选用 None 模型; 动区域与静区域之间设置为动静交界面, 选用 Frozen rotor 模型。流体模型选用  $k-\epsilon$  湍流模型, 求解格式选择 High Resolution, 收敛残差设置为  $10^{-4}$ , 设置完成后进行数值模拟的求解计算。

## 2 潜水搅拌机流场分析

为了研究搅拌池内液体在不同叶片安放角度下流场的变化, 现分别选取叶片安放角度为  $-4^\circ$ 、 $0^\circ$ 、 $4^\circ$  作为研究对象 (以  $0^\circ$  为基准, 考虑到叶片安放角为  $-2^\circ$  和  $2^\circ$  时在矢量图中的流速变化不太容易区分, 故选取以上 3 种角度变化作分析), 模拟计算完成后以  $Y=0$  作为研究平面, 对不同叶片安放角度下潜水搅拌器的速度流场进行对比分析。

从图 4 可以看出, 在 3 种不同的叶片安放角度下得到的速度矢量图大体趋势相似, 搅拌池内的速度流场关于潜水搅拌机呈现出轴对称性, 且沿潜水搅拌器的中心向前推流, 中心射流运动到另一边水池池壁附近时, 流体向四周扩散。对于流速大小分布而言, 在  $Y=0$  平面上中心线处的流速最大, 离中心线越远速度越小。但是, 速度矢量图中的射流扩散半径和形成的旋涡位置及大小有一定的区别。当叶片安放角为  $-4^\circ$  时, 自叶轮叶片工作面射出后的中心流体轴面速度要大于角度为  $0^\circ$  和  $4^\circ$ , 流场关于潜水搅拌器的轴对称性最好。同时, 叶片安放角为负角度下, 中心流体径向扩散受到了一定的压缩, 射流中心向前推进距离更远, 所以在接近另一侧池壁附近中心流速相较于  $0^\circ$  和  $4^\circ$  时更大, 相应地回流与射流形成的旋涡位置离潜水搅拌机也就越远。这说明当叶片安装角逐渐增大时, 对周围流体的吸引作用更大, 致使形成旋涡区的位置更靠前, 回流区域的范围更广。

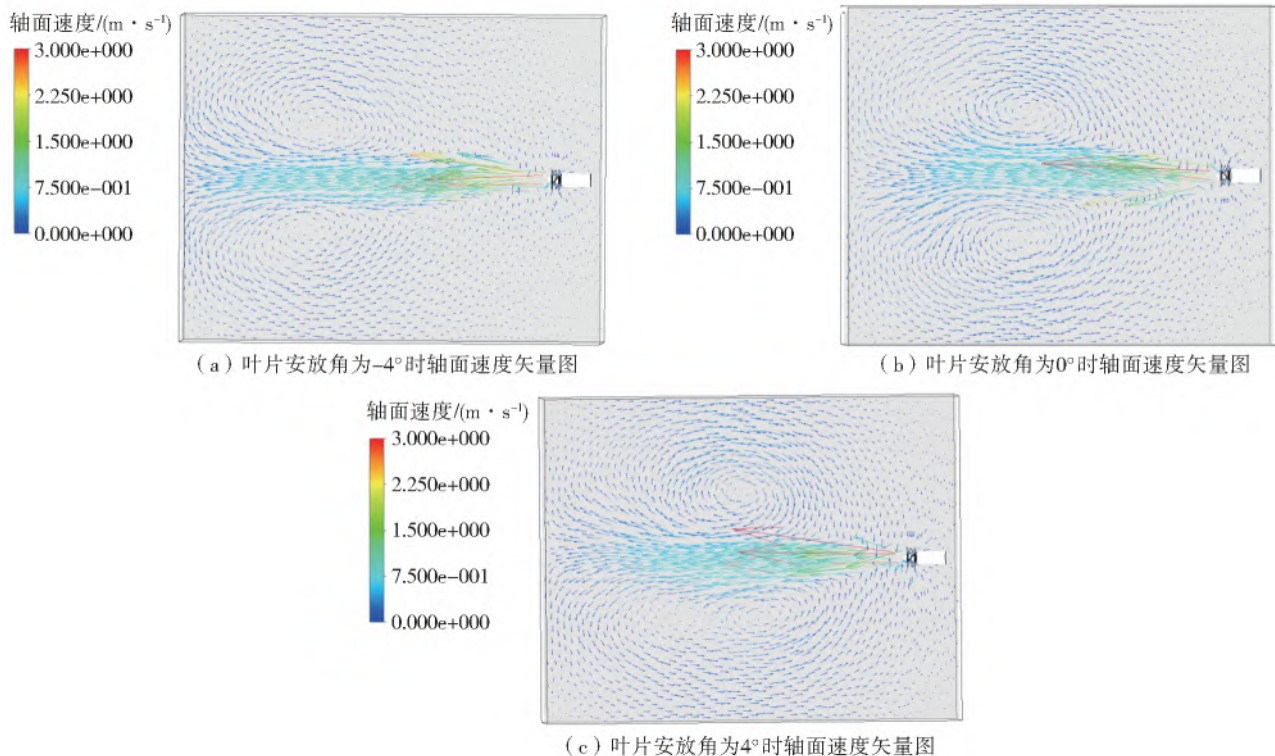


图 4 不同叶片安放角下潜水搅拌器的轴面速度矢量图

Fig. 4 Axial velocity vector diagram of submersible agitator with different blade angle

图 5 为 3 种不同叶片安装角下潜水搅拌器的横截面速度分布云图。在同一图例标尺下, 潜水搅拌器的流场呈现出了一定的对称性, 这也与图 4 的速度矢量图相对应。但是在潜水搅拌器的安装侧, 水池的四周和出现旋涡的区域因为流速较慢, 所以出现了较为明显的低速区。对比 3 幅速度云图可知, 潜水搅拌机在不同叶片安放角下得到的有效搅拌区

域大小关系是:  $4^\circ > 0^\circ > -4^\circ$ , 且叶片安放角为  $4^\circ$  时在潜水搅拌机安装侧流速  $\geq 0.08$  m/s 搅拌范围更大。从图 5 还可以看出, 当叶片安放角为  $0^\circ$  和  $4^\circ$  时, 在潜水搅拌机下部流场旋涡后面又出现一个小的低速回流区, 原因可能是叶片角度逐渐增大的情况下形成的旋涡位置更靠前, 且越接近潜水搅拌机安装侧总体流速越大, 一部分流体不足以被全部抵



消掉形成旋涡,进而继续向后运动,与碰到池壁后形成的回流方向相反,两种速度相互扰动、抵消,故形成了一个流速大于旋涡的低速回流区。但总体而

言,随着潜水搅拌机叶片安放角的增大,有效搅拌区域的面积越来越大,对搅拌池内流场的影响越来越优越。

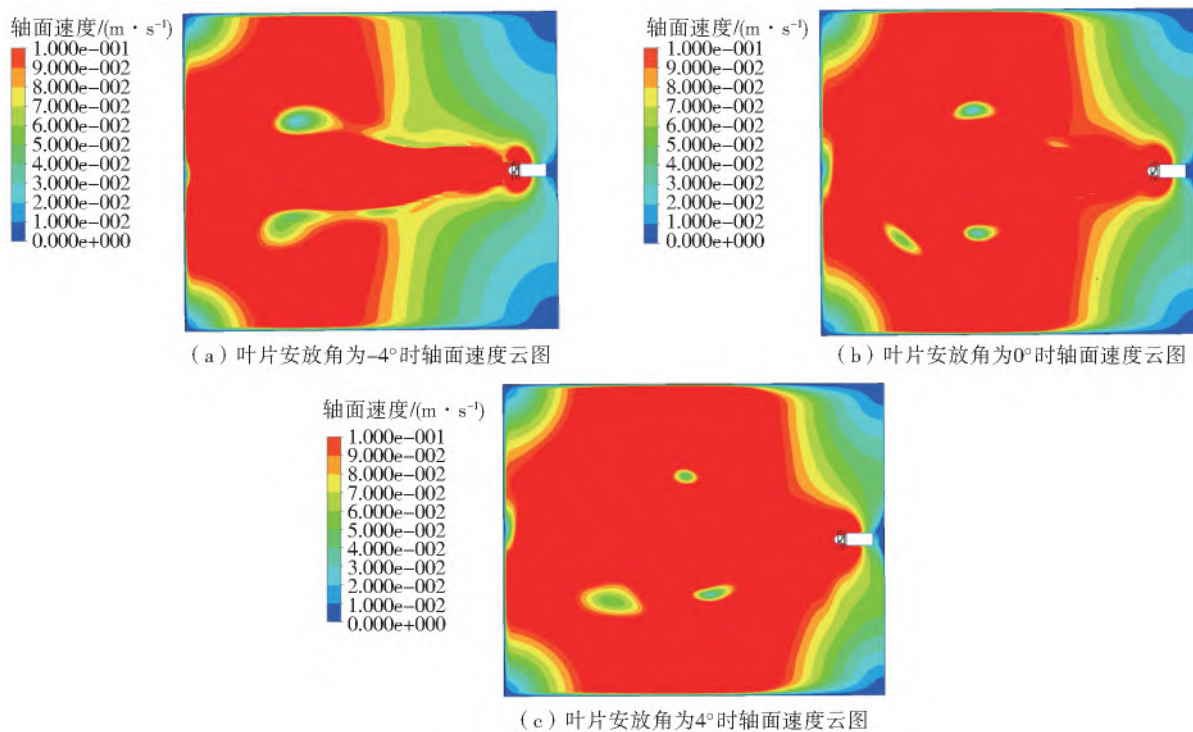


图 5 不同叶片安放角下潜水搅拌器的轴面速度分布云图

Fig. 5 Cloud chart of axial velocity distribution of submersible agitator under different blade angle

### 3 潜水搅拌机外特性参数分析

观察图 6 可以发现,在不同叶片安放角下叶轮压力面压力分布特点几乎是一致的,即高压区主要集中在叶轮进口区域的位置,负压区集中在叶片轮缘和叶轮出口附近区域。潜水搅拌机叶片安放角为 $-4^\circ$ 时叶片工作面高压区的面积占叶片整体面积较小,当叶片安放角由 $-4^\circ$ 增加到 $4^\circ$ 时,高压区域的面

积由入口位置逐渐向中部及出口位置延伸扩大,当叶片安放角为 $4^\circ$ 时,叶片高压区面积已经占据了整个叶片的二分之一以上,说明随着叶片安放角的增加,叶片工作面所受压强增大,即高压区面积不断地增加。但是,叶轮压力面的负压区域的大小和位置基本没有变化。取不同叶片安放角下潜水搅拌器的轴功率和推力,见表 1。

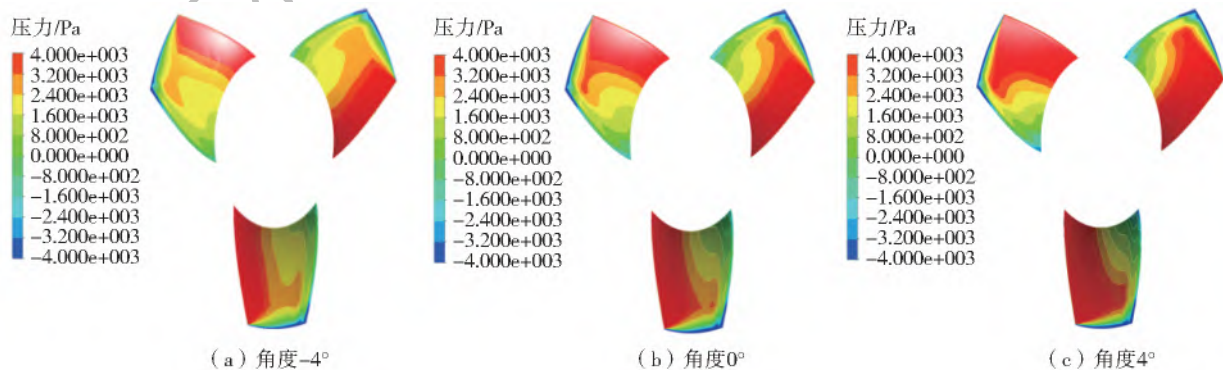


图 6 不同叶片安放角下潜水搅拌机叶轮压力面云图

Fig. 6 Cloud chart of pressure surface of submerged agitator impeller under different blade angle

从表 1 可以看出,随着叶片安放角的增大,潜水搅拌器的轴功率和推力呈现出不断增加的趋势。当叶片安放角为 $-4^\circ$ 时,潜水搅拌机轴功率和推力最

小;当叶片安放角为 $4^\circ$ 时,轴功率和推力达到最大值。因为叶片安放角在 $-4^\circ$ 时,叶片表面所受的压强也就越小,随着叶片

安放角增加到 $4^\circ$ ,作用力也随之不断增加,压强也就越来越大。这也和图6中叶片安放角为 $-4^\circ$ 时压力面高压区面积最小,叶片安放角为 $4^\circ$ 时压力面高压区面积最大相对应。这种变化表现在流场中就是随着叶片安放角的不断增加,搅拌池内的搅拌区域越来越广。

表1 不同叶片安放角下轴功率和推力  
Tab.1 Shaft power and thrust under different blade placement angles

安放角度	$-4^\circ$	$-2^\circ$	$0^\circ$	$2^\circ$	$4^\circ$
轴功率/W	490.55	580.46	686.56	817.43	956.27
推力/N	232.64	256.52	279.85	303.18	325.62

现以整个搅拌池为研究对象,进行取点分析观察不同位置下的轴向流速变化。以水池正中央A点为坐标原点,记为 $S=0$ ;B点为沿Z轴方向从A点向远离潜水搅拌机安装侧平移1m,记为 $S=1$ m;C点为沿Z轴方向从A点向远离潜水搅拌机安装侧平移2m,记为 $S=2$ m。 $H$ 表示布线位置的深度(Y轴方向),即A和D两点间的垂直距离,记为 $H=0.2$ m,具体布点情况见图7。

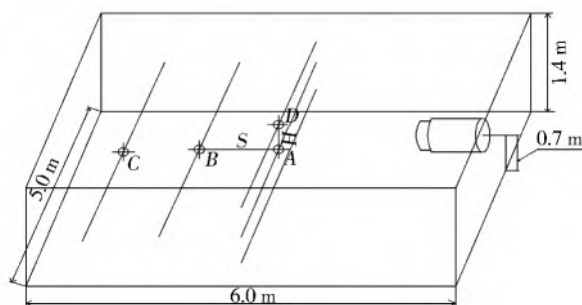


图7 潜水搅拌机水池布点

Fig.7 Distribution diagram of submersible agitator pool

图8反映了在 $S=0$ 、 $H=0$ (A点)情况下的轴向速度变化,可以看出:不管叶片安放角怎么改变,流场的流速变化趋势基本一致,均在中心零点处达到最大速度值,从射流中心沿径向往水池两边靠近,轴向流速逐渐衰减为 $0$  m/s,继续靠近,流速变为与射流方向相反的速度。其中,叶片安放角为 $-4^\circ$ 时在零点处流速值最大,轴向流速往水池两边的衰减也最快,并且随着叶片安放角由 $-4^\circ$ 增大为 $4^\circ$ ,射流中心的轴向流速径向衰减逐渐变慢。

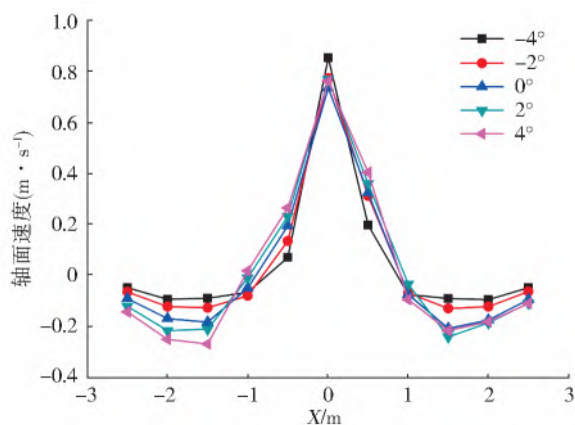


图8 不同叶片安放角下同一推进距离处轴向流速曲线  
Fig.8 Curve of axial velocity at the same propulsion distance under different blade angles

如图9取3种叶片安放角下 $S=0$ (A点)、 $S=1$ m(B点)和 $S=2$ m(C点)不同推进距离时的轴向流速变化曲线图分析比较:在同一叶片安放角下,随着推进距离 $S$ 的不断增大,中心流速不断地减小,且射流中心的轴向流速随着推进距离 $S$ 的增加径向衰减逐渐变慢。叶片安放角为 $-4^\circ$ 时轴向流速关于射流中心的对称性变化最好,这与图4的矢量图和图5的云图表现相一致。

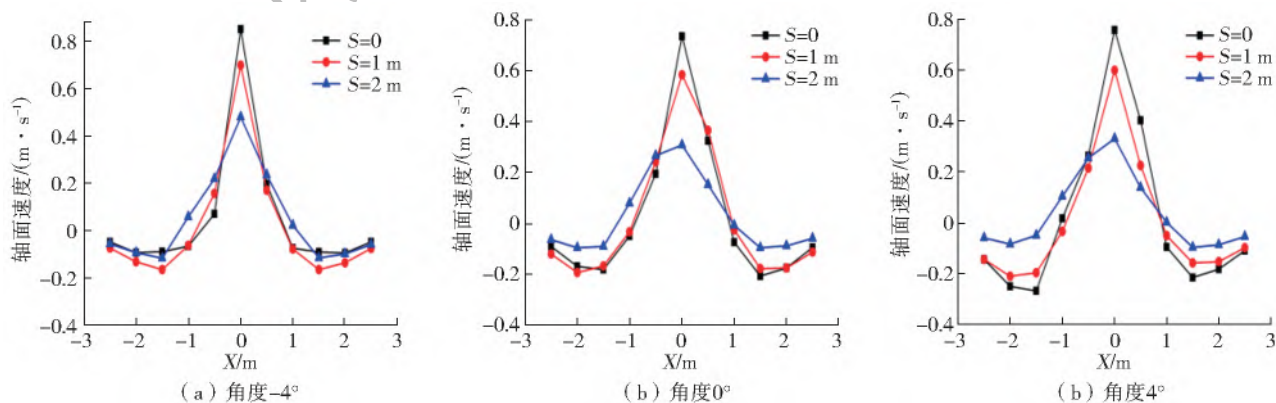


图9 不同叶片安放角时推进距离轴向速度流场( $H=0$ )

Fig.9 Flow field of axial velocity of propulsion distance with different blade angle( $H=0$ )

#### 4 潜水搅拌机搅拌效果分析

潜水搅拌机搅拌效果计算公式为

$$\eta = V_1 / V_2 \quad (1)$$

$$P_2 = P_1 / V_1 \quad (2)$$

式中: $\eta$ 为搅拌池的有效搅拌比,%; $V_1$ 为搅拌池中

流速( $v \geq 0.08 \text{ m/s}$ )的流体体积,  $\text{m}^3$ ;  $V_2$  为搅拌池的体积,  $\text{m}^3$ ;  $P_1$  为潜水搅拌器的电机功率,  $\text{W}$ ;  $P_2$  为达到搅拌要求的流体的有效单位能耗,  $\text{W}/\text{m}^3$ ;  $V_1$  为达到搅拌要求的流体体积,  $\text{m}^3$ 。

在 CFD-Post 后处理软件中将流速( $v \geq 0.08 \text{ m/s}$ )达到要求的流体体积取出来, 并根据式(1)和式(2)计算出潜水搅拌器的有效搅拌比和有效单位能耗, 见表 2。

表 2 不同叶片安放角下有效搅拌比和有效单位能耗

Tab. 2 Effective mixing ratio and effective unit energy consumption under different blade placement angles

安放角度	$-4^\circ$	$-2^\circ$	$0^\circ$	$2^\circ$	$4^\circ$
$\eta/\%$	49.61	56.03	63.30	66.50	69.64
$P_2/(\text{W} \cdot \text{m}^{-3})$	23.54	24.67	25.82	29.27	32.69

从表 2 可以看出, 潜水搅拌器的有效搅拌比和有效单位能耗均随着叶片安放角的增大不断地增大。当叶片安放角为  $-4^\circ$  时, 潜水搅拌器的有效单位能耗最小, 搅拌池内的有效搅拌区域也有一半左右, 流场中会出现一部分低速区甚至死区, 影响搅拌效果; 当叶片安放角增大到  $4^\circ$  时, 潜水搅拌器的搅拌区域已达 70% 左右(实际工程应用中潜水搅拌器搅拌效果已达到 70% 作为搅拌性能良好的标准), 流场中大部分流体已处于搅拌中, 满足了设计要求, 搅拌效果较好, 从图 4 的矢量图和图 5 的云图中能更真切地看到这种变化。所以, 工程设计中可以根据自身需求选择相应的叶片安放角度。

### 5 试验验证

针对以上数值模拟的情况, 为了更好地有利于试验的进行, 选取叶片安放角为  $0^\circ$  时进行试验验证。试验安装情况见图 10。



图 10 潜水搅拌器试验

Fig. 10 Test drawing of submersible agitator

根据图 11 潜水搅拌器测量原理, 得到潜水搅拌器的试验测量公式为

$$F_1 \times l_1 = F_2 \times (l_1 + l_2) \quad (3)$$

$$M_1 + F_3 \times l_2 = 0 \quad (4)$$

式中:  $F_1$  为潜水搅拌器产生的水推力,  $\text{N}$ ;  $F_2$  为测量推力传感器的拉力,  $\text{N}$ ;  $F_3$  为测量扭矩传感器的拉力,  $\text{N}$ ;  $l_1$  为轴承底座到潜水搅拌器轴线的垂直距离,  $\text{m}$ ;  $l_2$  为潜水搅拌器轴线到测量拉力传感器轴线的垂直距离,  $\text{m}$ ;  $M_1$  为潜水搅拌器的扭矩,  $\text{N} \cdot \text{m}$ 。

当潜水搅拌器转速为  $576 \text{ r/min}$  时进行试验, 得到潜水搅拌器的实际功率(多次试验取平均值)为  $658.8 \text{ W}$ , 功率相对误差为  $4.21\%$ , 数值模拟和试验验证的结果误差在  $5\%$  以内, 证明了数值模拟结果的准确性, 说明关于潜水搅拌器叶片安放角的研究具有可行性。

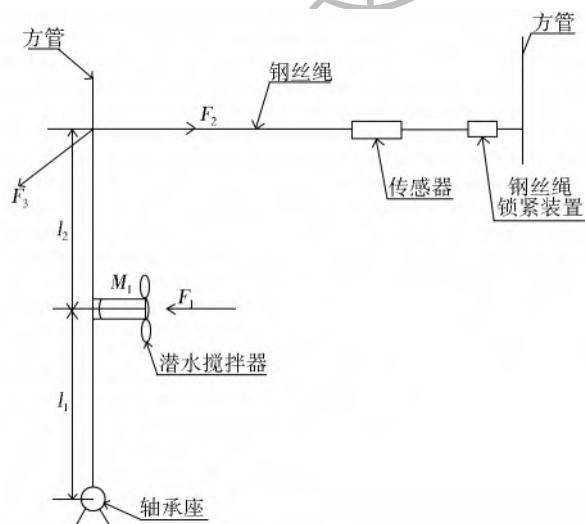


图 11 潜水搅拌器测量原理

Fig. 11 Measuring principle diagram of submersible agitator

### 6 结论

(1) 在不同叶片安放角下所得到的潜水搅拌器速度矢量图均呈现出轴向推进、径向扩散的现象, 且随着叶片安放角的不断增大, 搅拌池内流速分布云图达到有效搅拌的面积越来越大, 说明搅拌性能越来越好。

(2) 当叶片安放角由  $-4^\circ$  增加到  $4^\circ$  时, 潜水搅拌器电机的轴功率和推力不断地增大, 叶片压力面的高压区面积也在持续递增。在不同叶片安放角下流场流速的变化趋势一致, 其中在  $-4^\circ$  时射流中心轴向速度值最大。同时, 随着潜水搅拌器叶片安放角的增大, 对应的有效搅拌比和有效单位能耗也在不断地增加。

(3) 通过试验发现潜水搅拌器功率实际值与理论值的相对误差在  $5\%$  以内, 验证了数值模拟结果的准确性与合理性。



## 参考文献(References):

- [1] 严建华,黄道见,滕国荣. 潜水搅拌机在处理农村生活污水中的应用[J]. 安徽农业科学, 2009, 37(20): 9606-9607, 9628. (YAN J H, HUANG D J, TENG G R. Application of submersible agitator in rural domestic sewage treatment [J]. An hui Agricultural Science, 2009, 37(20): 9606-9607, 9628. (in Chinese)) DOI: 10. 13989/j. cnki. 0517-6611. 2009. 20. 017
- [2] 伍伟强. 浅谈污水处理厂潜水搅拌器的选型[J]. 中国科技信息, 2008(9): 116, 118. (WU W Q. Selection of submersible agitator in sewage treatment plant [J]. China Science and Technology Information, 2008(9): 116, 118. (in Chinese))
- [3] 蔡芝斌,姚斌,邹华. 绍兴污水处理厂进口潜水搅拌机应用与维修[J]. 给水排水, 2012, 48(2): 93-95. (CAI Z B, YAO B, ZOU H. Application and maintenance of imported submersible agitator in Shaoxing sewage treatment plant[J]. Water Supply and Drainage, 2012, 48(2): 93-95. (in Chinese)) DOI: 10. 13789/j. cnki. wwe1964. 2012. 02. 013.
- [4] 王显,高卫东. 潜水搅拌机在污水处理领域中的应用[J]. 给水排水, 1997(2): 52-53. (WANG X, GAO W D. Application of submersible agitator in sewage treatment [J]. Water Supply and Drainage, 1997(2): 52-53. (in Chinese)) DOI: 10. 13789/j. cnki. wwe1964. 1997. 02. 016.
- [5] 田飞,施卫东,卢熙宁,等. 污水处理潜水搅拌机效率的理论计算与模拟分析[J]. 农业工程学报, 2012, 28(12): 50-54. (TIAN F, SHI W D, LU X N, et al. Theoretical calculation and simulation analysis of efficiency of submersible mixer for sewage treatment [J]. Journal of Agricultural Engineering, 2012, 28(12): 50-54. (in Chinese)) DOI: 1002-6819 (2012) -12-0050-05.
- [6] 马佳骏. 污水处理厂改造工程中搅拌机选用比较与效果[J]. 上海水务, 2008(3): 18-19. (MA J J. Comparison and effect of agitator selection in sewage treatment plant reconstruction project [J]. Shanghai Water, 2008(3): 18-19. (in Chinese))
- [7] 易春林,翟红卫. 潜水搅拌机在污水处理领域中的应用[J]. 漯河职业技术学院学报(综合版), 2003(2): 17-18. (YI C L, ZHAI H W. Application of submersible agitator in sewage treatment [J]. Journal of Luohe Vocational and Technical College (Comprehensive Edition), 2003(2): 17-18. (in Chinese))
- [8] 徐伟幸,袁寿其. 基于 FLUENT 的潜水搅拌机搅拌流场分析[J]. 机械设计与制造, 2011(9): 155-157. (XU W X, YUAN S Q. Flow field analysis of submersible agitator based on FLUENT [J]. Mechanical Design and Manufacturing, 2011(9): 155-157. (in Chinese)) DOI: 10. 19356/j. cnki. 1001-3997. 2011. 09. 058.
- [9] 徐伟幸,袁寿其. 基于搅拌流场分析的潜水搅拌机优化设计及工程应用[J]. 中国农村水利水电, 2011(6): 32-35. (XU W X, YUAN S Q. Optimization design and engineering application of submersible agitator based on mixing flow field analysis [J]. China Rural Water and Hydropower, 2011(6): 32-35. (in Chinese))
- [10] 徐伟幸. 潜水搅拌机叶轮设计及搅拌流动研究[J]. 煤炭技术, 2011, 30(9): 207-208. (XU W X. Design of submersible agitator impeller and study of mixing flow [J]. Coal Technology, 2011, 30(9): 207-208. (in Chinese))
- [11] 刘晓满. 潜水搅拌机水力特性的优化研究[D]. 北京: 北京建筑工程学院, 2012. (LIU X M. Study on optimization of hydraulic characteristics of submersible agitator [D]. Beijing: Beijing Institute of Architecture and Engineering, 2012. (in Chinese))
- [12] 徐顺,汤方平,汤超,等. 潜水搅拌机选型影响因子及其优化研究[J]. 中国给水排水, 2016, 32(23): 76-79. (XU S, TANG F P, TANG C, et al. Study on influencing factors and optimization of submersible agitator selection [J]. China Water Supply and Drainage, 2016, 32(23): 76-79. (in Chinese))
- [13] 徐顺,汤方平,汪文生,等. 叶片间隙对潜水搅拌机流场特性的影响[J]. 中国给水排水, 2017, 33(1): 106-109. (XU S, TANG F P, WANG W S, et al. Effect of blade clearance on flow field characteristics of submersible agitators [J]. China Water Supply and Drainage, 2017, 33(1): 106-109. (in Chinese))
- [14] 张晓宁,赵静野,王文海. 潜水搅拌机安装角度对搅拌效果的影响[J]. 北京建筑大学学报, 2014, 30(4): 48-51. (ZHANG X N, ZHAO J Y, WANG W H. Influence of installation angle of submersible mixer on mixing effect [J]. Journal of Beijing University of Architecture, 2014, 30(4): 48-51. (in Chinese))
- [15] 龚发云,潘明铮,汤亮. 基于 FLUENT 的潜水搅拌机数值模拟[J]. 湖北工业大学学报, 2017, 32(1): 93-96. (GONG F Y, PAN M Z, TANG L. Numerical simulation of submersible agitator based on fluent [J]. Journal of Hubei University of Technology, 2017, 32(1): 93-96. (in Chinese))
- [16] 许乔. 基于搅拌流场特性的潜水搅拌机叶轮设计研究[D]. 扬州: 扬州大学, 2018. (XU Q. Research on the design of submersible agitator impeller based on the characteristics of mixing flow field [D]. Yangzhou: Yangzhou University, 2018. (in Chinese))
- [17] 徐莹,汤方平,许乔. 基于轴流泵叶轮设计的潜水搅拌机特性分析[J]. 中国农村水利水电, 2019(4): 178-182. (XU Y, TANG F P, XU Q. Characteristic analysis of submersible agitator based on axial-flow pump impeller design [J]. China Rural Water and Hydropower, 2019(4): 178-182. (in Chinese))

- [18] 朱桂华,彭南辉,张傲林,等. 潜水搅拌机安装角度对盐泥水洗搅拌效果的影响[J]. 西安交通大学学报, 2019, 53(7): 16-22, 59. (ZHU G H, PENG N H, ZHANG A L, et al. Influence of installation angle of submersible agitator on mixing effect of salt mud water washing[J]. Journal of Xi'an Jiaotong University, 2019, 53(7): 16-22, 59. (in Chinese)) DOI: 10. 7652/xjtub201907003.
- [19] 施卫东,田飞,曹卫东,等. 不同池形中推流搅拌机功率消耗的数值模拟[J]. 排灌机械, 2009, 27(3): 140-144. (SHI W D, TIAN F, CAO W D, et al. Numerical simulation of power consumption of push flow agitators in different pool shapes[J]. Irrigation and Drainage Machinery, 2009, 27(3): 140-144. (in Chinese))
- [20] 肖夏,冯岚,刘雪垠. 基于 CFX 的某型推流式潜水搅拌机导流罩位置对工作效率的影响[J]. 机械, 2019, 46(7): 71-75. (XIAO X, FENG L, LIU X Y. The influence of the position of the flow guide cover on the working efficiency of a certain type of push flow submersible mixer based on CFX[J]. Machinery, 2019, 46(7): 71-75. (in Chinese)) DOI: 10. 3969/j. issn. 1006-0316. 2019. 07. 015.
- [21] 田飞,施卫东,张德胜,等. 新型多叶轮潜水搅拌机流场特性[J]. 排灌机械工程学报, 2019, 37(3): 232-236. (TIAN F, SHI W D, ZHANG D S, et al. Flow field characteristics of a new multi impeller submersible mixer[J]. Journal of Drainage and Irrigation Machinery Engineering, 2019, 37(3): 232-236. (in Chinese)) DOI: 10. 3969/j. issn. 1674-8530. 18. 0201.
- [22] 田飞,施卫东,张启华,等. 2 叶片潜水搅拌机叶轮内部流场特性[J]. 江苏大学学报(自然科学版), 2013, 34(4): 395-398, 434. (TIAN F, SHI W D, ZHANG Q H, et al. Internal flow field characteristics of 2-Blade submersible mixer impeller[J]. Journal of Jiangsu University (Natural Science Edition), 2013, 34(4): 395-398, 434. (in Chinese)) DOI: 10. 3969/j. issn. 1671-7775. 2013. 04. 005.
- [23] 田飞,施卫东,卢熙宁,等. 三叶片潜水搅拌机的数值模拟[J]. 排灌机械工程学报, 2012, 30(1): 11-14. (TIAN F, SHI W D, LU X N, et al. Numerical simulation of three blade submersible mixer[J]. Journal of Drainage and Irrigation Machinery Engineering, 2012, 30(1): 11-14. (in Chinese)) DOI: 1674-8530 (2012) 01-0011-04.
- [24] 史书舟,王娅娜,谢敬革,等. CFD 模拟在潜水搅拌设备布置及工况优化中的应用[J]. 给水排水, 2019, 55(9): 36-40. (SHI S Z, WANG Y N, XIE J G, et al. Application of CFD simulation in layout and condition optimization of diving mixing equipment[J]. Water Supply and Drainage, 2019, 55(9): 36-40. (in Chinese)) DOI: 10. 13789/j. cnki. wwe1964. 2019. 09. 007.
- [25] 金建华,张红伟. 潜水搅拌机三维两相流的数值模拟[J]. 中国农村水利水电, 2014(10): 159-162. (JIN J H, ZHANG H W. Numerical simulation of three-dimensional two-phase flow of submersible mixer[J]. China Rural Water Conservancy and Hydropower, 2014(10): 159-162. (in Chinese))

### Performance analysis of blade angle of submersible agitator

REN Xiangxuan<sup>1</sup>, TANG Fangping<sup>2</sup>, XU Ying<sup>1</sup>, SHI Lijian<sup>2</sup>, SHANG Xiaojun<sup>3</sup>

(1. School of Electricity, Energy and Power Engineering, Yangzhou University, Yangzhou 225009, China;

2. School of Water Conservancy Science and Engineering, Yangzhou University, Yangzhou 225009, China;

3. Taihu Lake District Water Conservancy Management Office, Suzhou 215128, China)

**Abstract:** Submersible agitator, also known as submersible propeller, is widely used in the sewage treatment plant process. Recently, the use of CFD software is used to simulate the flow field changes in the stirred tank, more clearly provides us with theoretical support. It is the emergence of this numerical simulation technology that the research of submersible agitators has entered a new stage. Therefore, researchers from the design parameters of the submersible mixer, installation position, speed adjustment, and other aspects, to not only improve the mixing effect of the submersible mixer, but also achieve the purpose of effective energy saving.

Up to now, the installation scheme of submersible agitators has been studied more or less. However, how the blade angle of the submersible agitator affects the flow field has not been studied. Therefore, based on the previous research, the influence of blade angle on the performance of submersible agitators is simulated. The change of impeller blade setting angle is realized by rotating the corresponding angle around the  $y$ -axis in turbogrid. The  $y$ -axis rotates  $2^\circ$  in the positive direction (clockwise), that is, the blade setting angle is adjusted to  $-2^\circ$  (clockwise is negative, counterclockwise is positive), and so on. The purpose is to study the flow characteristics in the stirred tank with different blade placement angles ( $-4^\circ$ ,  $-2^\circ$ ,  $0^\circ$ ,  $2^\circ$  and  $4^\circ$ ), to provide a reference for selecting the appropriate blade placement angle according to the mixing requirements and energy-saving effect.

To study the influence of different blade angles ( $-4^\circ$ ,  $-2^\circ$ ,  $0^\circ$ ,  $2^\circ$  and  $4^\circ$ ) on the flow field in the stirred tank, the numerical simulation of the submerged agitator with different blade angles is carried out, and the flow field is analyzed by CFD-Post soft-



ware. According to the results of numerical simulation, it is concluded that: (1) The velocity field in the mixing tank is axisymmetric concerning the submersible agitator. The flow is pushed forward along the center of the submersible agitator. When the central jet moves to the other side of the tank wall, the flow diffuses around. The area of velocity distribution cloud diagram in the mixing tank to achieve effective mixing becomes larger and larger with the increase of blade angle, which indicates that the mixing effect of submersible agitator becomes better and better when the blade angle increases from  $-4^\circ$  to  $4^\circ$ . (2) The pressure distribution characteristics of the impeller pressure surface are almost the same under different blade placement angles, that is, the high-pressure area is mainly concentrated in the inlet area of the impeller, and the negative pressure area is concentrated in the area near the blade flange and impeller outlet. The pressure on the blade working surface increases with the increase of blade placement angle, that is, the area of the high-pressure area increases continuously. At the same time, the shaft power and thrust of the submersible agitator are increasing with the increase of blade angle. (3) Compared with the mixing effect, the effective mixing ratio and effective unit energy consumption of submersible agitators increase with the increase of blade angle. When the blade angle is  $-4^\circ$ , the effective unit energy consumption of the submersible mixer is the minimum, and the effective mixing area in the mixing tank is only about half, and a part of low-speed zone or even dead zone will appear in the flow field, which affects the mixing effect. When the blade angle is increased to  $4^\circ$ , the mixing area of the submersible mixer is about 70% (the mixing effect of the submersible mixer has been improved in practical engineering application). Most of the fluid in the flow field has been stirred, which meets the design requirements, and the stirring effect is good. (4) Finally, to prove the accuracy of the numerical simulation results of submersible agitator, the experimental verification is carried out when the blade setting angle is  $0^\circ$  and the error between the numerical simulation and experimental verification is less than 5%, which proves the accuracy of the numerical simulation results. It shows that the research on the blade setting angle of the submersible agitator is feasible and provides a reference for the future research of submersible agitator certain reference.

**Conclusions** (1) With the increase of blade angle, the effective mixing area of velocity distribution nephogram in the mixing tank is increasingly larger, and the mixing performance of submersible agitator is improved. (2) When the blade angle increases from  $-4^\circ$  to  $4^\circ$ , the shaft power and thrust of submersible agitator motor increase continuously. At the same time, with the increase of blade angle, the corresponding effective mixing ratio and effective unit energy consumption are also increasing. (3) The accuracy and rationality of the numerical simulation results are verified by experiments, which provides certain reference for the future research of submersible agitator.

**Key words:** submersible agitator; blade angle; numerical simulation; axial velocity

(上接第 794 页)

agreed well with the measured data with the same trend. The displacement of the Xiaowan arch dam was closely related to the upstream water level. The dam had a trend of slow deformation to the downstream because the aging effect had not yet fully converged at present. (4) The upstream dam surface was basically in a pressure state. Besides, the maximum compressive stress, which was located at the height of 975 m, was about 10 MPa. However, the dam surface above the water level was under tension in winter, and the maximum tensile stress was about 0.6 MPa. The downstream dam surface was basically in a compressive state, and the maximum compressive stress could reach to 17.3 MPa, which was located at the dam toe. Besides, the tensile stress zone appeared near the interface between the dam body and the foundation due to the stress concentration, and the global maximum tensile stress was about 0.8 MPa, although the operating state of the dam was still in the safe scope.

**Conclusions** (1) The temperature of the downstream dam surface was mainly affected by atmospheric temperature, showing a phenomenon that the temperature was higher on both sides than the middle section. (2) The elastic modulus of the dam concrete during the operation was increased by about 30% relative to the test value. (3) The stress distributions of the Xiaowan arch dam revealed that its operating state was still in the safe scope.

**Key words:** Xiaowan arch dam; temperature field; material parameters; inverse analysis; stress simulation